Resting State Conformation of the MsbA Homodimer As Studied by Site-Directed Spin Labeling

Adam H. Buchaklian, Andrea L. Funk, and Candice S. Klug*

Department of Biophysics, Medical College of Wisconsin, 8701 Watertown Plank Road, Milwaukee, Wisconsin 53226

Received January 30, 2004; Revised Manuscript Received May 6, 2004

ABSTRACT: MsbA is the ABC transporter for lipid A and is found in the inner membranes of Gram-negative bacteria such as *Escherichia coli*. Without MsbA present, bacterial cells accumulate a toxic amount of lipid A within their inner membranes. A crystal structure of MsbA was recently obtained that provides an excellent starting point for functional dynamics studies in membranes [Chang, and Roth (2001) *Science 293*, 1793−1800]. Although a structure of MsbA is now available, many questions remain concerning its mechanism of transport. Site-directed spin labeling (SDSL) electron paramagnetic resonance (EPR) spectroscopy is a powerful approach for characterizing local areas within a large protein structure in addition to detecting and following changes in local structure due to dynamic interactions within a protein. The quaternary structure of the resting state of the MsbA homodimer reconstituted into lipid membranes has been evaluated by SDSL EPR spectroscopy and chemical cross-linking techniques. SDSL and cross-linking results are consistent with the controversial resting state conformation of the MsbA homodimer found in the crystal structure, with the tips of the transmembrane helices forming a dimer interface. The position of MsbA in the membrane bilayer along with the relative orientation of the transmembrane helical bundles with respect to one another has been determined. Characterization of the resting state of the MsbA homodimer is essential for future studies on the functional dynamics of this membrane transporter.

Multidrug resistance (MDR) is becoming an increasingly serious problem in a number of areas of medicine, especially in the treatment of infectious diseases and cancer (*1*−*7*). ATP binding cassette (ABC) transporters aid in drug resistance by using ATP hydrolysis to translocate drugs back across the cell membrane. In addition, serious genetic disorders such as cystic fibrosis (*8*) also result from the function or dysfunction of ABC transporters.

Human MDR transporters such as MDR1 (*9*), a P-glycoprotein, are known to be able to transport an array of various drugs (*10*). Their ability to not only transport drugs or phospholipids but also to "flip" them 180° has given rise to names such as flippases and hydrophobic vacuum cleaners (e.g., *11*). MDR transporters generally include two membrane spanning domains and two intracellular ATP binding domains (nucleotide binding domains, NBDs), either all on one gene [e.g., human MDR1 (*9*) and the cystic fibrosis transmembrane conductance regulator (*8*)] or as a homodimer [e.g., MsbA (*11*, *12*)]. To better understand the MDR transporters, several crystal structures of various MDR ABC transporters have been solved, including MsbA (*11*, *12*), MalK (*13*), and HisP (*14*). The structures reveal that the ATP binding domains typically form at least one of the dimer interfaces, that each NBD binds one ATP molecule, and that the transmembrane domains are either attached as six helix bundles [as in MsbA (*11*, *12*), P-glycoprotein (*15*), and Rad50 (*16*)] or contained in tightly bound separate proteins such as is the case with the $MalFGK_2$ (*17*) and histidine permease (*18*) complexes. In all cases, the dimer form is necessary for activity, indicating that cooperativity between the two subunits is essential.

MsbA is the ATPase lipid A transporter found in the inner membranes of Gram-negative bacteria such as *Escherichia coli*. MsbA derived from *E. coli* is comprised of 582 amino acids with a monomeric molecular mass of 65 kDa (*19*). MsbA loss from the cell results in a toxic accumulation of lipid A in the inner membrane (*20*), making it the only bacterial ABC transporter that is required for bacterial viability (*21*). Because lipid A is the major component of the outer leaflet of the outer membrane of Gram-negative bacteria, its synthesis and transport are also essential for cell growth.

A crystal structure of the *E. coli* MsbA homodimer was recently solved to a resolution of 4.5 Å (*11*). The structure reveals that the MsbA monomer contains a transmembrane six helix bundle linked to a globular NBD by a short four helix bundle. As most, if not all, inner membrane proteins are α-helical and ATPases by definition contain NBDs, the structure itself was not surprising. However, the dimer structure with the periplasmic tips of the helical bundles comprising the dimer interface and the NBDs > 40 Å apart has triggered controversy regarding the implied physiological relevance of this dimer structure (*22*−*24*). The few other ATPases that have been crystallized, such as MalK (*13*), Rad50 (*16*), and HisP (*14*), all have their NBDs involved in the dimer interfaces. Because the buried surface area found in the crystallographic MsbA dimer is considerably less than

* To whom correspondence should be addressed. Tel: 414-456-4015. Fax: 414-456-6512. E-mail: candice@mcw.edu.

10.1021/bi0497751 CCC: $27.50
Published on Web 06/08/2004

that typically found necessary for a stable interface for proteins of this size, combined with the fact that other proteins in its class dimerize at their NBDs, the possibility arises that this dimer structure is a consequence of crystallization conditions and that another dimer arrangement forms the resting state of MsbA in its native membrane environment (e.g., *22*). The studies described here directly address the existence and orientation of the suggested dimer interface in a reconstituted membrane environment.

SDSL[1] EPR spectroscopy is a powerful tool that can provide a great deal of information on the location and environment of an individual residue within a very large and complex protein structure (*25*−*29*). Unlike other methods that allow only the monitoring of global changes in protein structure, SDSL allows the direct probing of the local environment, structure, and proximity of individual residues. Because EPR is not limited by either the macromolecular size or the optical properties of the sample, it is especially amenable to the investigation of membrane proteins, as they are normally difficult to study by other spectroscopy methods and are an important and large class of biologically relevant structures. The EPR spectroscopy technique has the unique ability to address and answer questions not solvable by genetic or crystal structure analysis and is especially amenable to the study of MsbA.

EXPERIMENTAL PROCEDURES

Materials. All lipids were purchased from Avanti Polar Lipids (Alabaster, AL). The nitroxide spin label MTSL was purchased from Toronto Research Chemicals (Ontario, Canada), the cross-linking agents were purchased from Pierce (Rockford, IL), and DM was obtained from Alexis Biochemicals (San Diego, CA).

Methods. Site-Directed Mutagenesis. The gene encoding the *E. coli* MsbA protein was obtained by polymerase chain reaction (PCR) amplification of the chromosomal copy from *E. coli* BL21 cells. The genomic DNA was purified from BL21 cells using the Wizard Genomic DNA Purification Kit (Promega). PCR amplification of the MsbA gene was carried out essentially as described previously (*30*). Briefly, forward and reverse primers were constructed that contained NdeI and BamHI sites and annealed to the initial and final sequences of the MsbA gene. These primers along with the genomic DNA as a template were used in a PCR reaction that produced a PCR product containing the MsbA gene flanked by the engineered NdeI and BamHI restriction sites, which was then digested and ligated into an NdeI/BamHI-cut pET28b vector (Novagen) creating a plasmid-encoded MsbA gene sequence with an N-terminal 6xHis-tag.

The two native cysteines, C88 and C315, were individually substituted with serine by site-directed mutagenesis using the QuikChange Mutagenesis Kit (Stratagene) in order to create the single cysteine mutations C88 (C88/C315S) and C315 (C88S/C315). In addition, both native cysteines were substituted with serines to create a cysteineless construct (C88S/C315S). Single cysteines were then individually introduced into the cysteineless MsbA to create the V29C, F56C, E133C, L171C, and A262C mutations. Mutant plasmids were sequenced by the MCW Protein and Nucleic Acid Facility (Milwaukee, WI) for verification of the introduced cysteine sequence.

Protein Purification. The plasmids containing the MsbA gene mutations were transformed into NovaBlue cells (Novagen) for protein purification. Five milliliters of an overnight culture started from a frozen stock and grown at 37 °C in Luria broth (LB) containing kanamycin (30 μg/mL) was subcultured into four 0.5 L flasks of LB/kanamycin and grown at 37 °C overnight with shaking. The cells were induced for 3 h with 1 mM isopropyl-1-thio-β-D-galactopyranoside (Fisher Scientific), pelleted, and washed. The cells were broken by a French press and pressure cell (Thermo-Spectronic), and the unbroken cells were pelleted by low speed centrifugation. The membrane fractions were collected by a high-speed centrifugation step and then solubilized in 1% DM (dodecylmaltoside). MsbA was purified by cobalt affinity chromatography using Talon resin (BD Biosciences Clontech) by elution with both 100 and 500 mM imidazole steps. Each fraction was monitored by SDS−PAGE, and the pure fractions were pooled and used immediately or stored frozen in 0.01% DM/50 mM $NaPO_4$/10% glycerol.

Spin Labeling and Lipid Reconstitution. MsbA mutants were labeled at a 10:1 molar ratio of the sulfhydryl specific spin label MTSL overnight at 4 °C. Excess label was removed by extensive dialysis against 50 mM $NaPO_4$, 0.01% DM, pH 7.0 buffer. Protein concentrations were determined by the detergent compatible DC Protein Assay (BioRad) using bovine serum albumin as a protein standard. The major phospholipids of the inner membrane of *E. coli* are PE, PG, and CL. These purified lipids in chloroform were mixed at a ratio of 65:25:10 PE:PG:CL, dried down under nitrogen, desiccated, and then resuspended and solubilized in 0.15% DM prior to the addition of MsbA at a protein:lipid molar ratio of 1:500. Biobeads (BioRad) were added to the mixture in order to remove the detergent. The resulting proteoliposome solution was then concentrated by high-speed centrifugation (30 min at 100000*g*) and resuspended in the desired volume of phosphate buffer (with or without NiEDDA or CROX).

Chemical Cross-Linking. Ten millimolar stock solutions in DMSO of BMOE (bis-maleimidoethane), DTME (dithio-bis-maleimidoethane), and DPDPB (dipyridyldithiopropionamidobutane) were made and added to 10 μM mutant MsbA reconstituted into lipids at a 10-fold molar excess for 2 h at room temperature. Each reaction was monitored by SDS−PAGE with monomeric MsbA run as a control.

Activity Assays. ATPase activities of each of the mutants and the WT protein were carried out using the EnzCheck Phosphate Assay Kit (Molecular Probes) following the manufacturer's instructions. Briefly, MsbA reconstituted into inner membrane lipids was incubated with 1000-fold excess ATP and assayed for the release of P_i by reaction with 2-amino-6-mercapto-7-methyl-purine riboside and purine nucleotide phosphorylase. Standard curves were generated using a KH_2PO_4 solution provided with the kit. All MsbA mutants tested showed activities similar to that of WT MsbA,

[1] SDSL, site-directed spin labeling; EPR, electron paramagnetic resonance; CW, continuous wave; NiEDDA, nickel ethylenediaminediacetic acid; CROX, potassium tris(oxalato)chromate or chromium oxalate; LGR, loop−gap resonator; SDS−PAGE, sodium dodecyl sulfate polyacrylamide gel electrophoresis; MTSL, methanethiosulfonate spin label; DM, dodecyl maltopyranoside; PE, phosphotidylethanolamine; PG, phosphotidylglycerol; CL, cardiolipin; DTT, dithiothreitol; WT, wild-type.

even in the absence of lipid A, similar to results shown previously for WT MsbA (*30*).

In addition, ATPase activity was carried out for purified WT MsbA in both detergent and in the presence of lipids containing lipid A. Using a colorimetric method previously described to measure the release of P_i (*31*), it was found that the basal activity gave a V_{max} of 10 nmol/min/mg and a K_m of 1445 μM, while the lipid-stimulated activities gave a V_{max} value of 35 nmol/min/mg and a K_m value of 1077 μM, showing a 3.5-fold stimulation in ATPase activity due to the presence of lipid A containing lipids. Spin-labeled WT MsbA (containing two labels per monomer in the lipid A binding pocket) was also tested for activity and showed an increase in basal activity (V_{max} of 13 nmol/min/mg and K_m of 1166 μM) and yet a slight decrease in lipid-stimulated activity (V_{max} of 25 nmol/min/mg and a K_m of 1556 μM) as compared to unlabeled WT protein.

EPR Spectroscopy. X-band CW EPR spectroscopy was carried out on a Bruker ELEXSYS fitted with a super high Q cavity, and the power saturation measurements were carried out on a Varian E-109 Century series spectrometer equipped with a LGR (Medical Advances, Milwaukee, WI). Samples were typically 50−100 μM protein and contained in a flame-sealed capillary or in a gas permeable TPX capillary for gas equilibration during accessibility measurements. Data were collected and analyzed using LabView data collection and analysis programs written by Christian Altenbach, Ph.D. (UCLA).

Accessibility of a spin label to a paramagnetic reagent decreases the effective spin−lattice relaxation time, T_1, resulting in an increase in the $P_{1/2}$ value. Thus, the more accessible a spin label is to a given paramagnetic reagent, the higher the $P_{1/2}$ value since the power required for saturation is increased due to collisions of the spin label with the paramagnetic relaxation reagent. Therefore, the change in $P_{1/2}$ ($\Delta P_{1/2}$) relative to a standard measured under N_2, for example, $P_{1/2}$ (O_2) − $P_{1/2}$ (N_2) = $\Delta P_{1/2}$ (O_2), is directly proportional to the bimolecular collision rate of the spin label with the paramagnetic probe (*32*). During power saturation experiments, the TPX capillary was equilibrated with a stream of either nitrogen or air (20% oxygen). The $P_{1/2}$ values for each sample in the presence of nitrogen, air, 175 mM NiEDDA, or 20 mM CROX (under nitrogen) were calculated as described by Altenbach et al. (*33*).

To estimate the depths of the spin label side chains in the membrane bilayer, the value Φ was calculated using the equation

$$\Phi = \ln[\Delta P_{1/2}\,(\text{air})/\Delta P_{1/2}\,(\text{NiEDDA})] \qquad (1)$$

and the depths were determined using the calibration equation:

$$\text{depth}\,(\text{Å}) = 4.73\Phi + 3.98 \qquad (2)$$

The inner membrane lipids containing unlabeled WT protein were calibrated for depth measurements with 5-, 7-, 10-, and 12-doxyl PC spin-labeled lipids. Φ values for each of the spin-labeled lipids were measured and plotted against known depths of the spin labels (*34*) resulting in the above calibration equation.

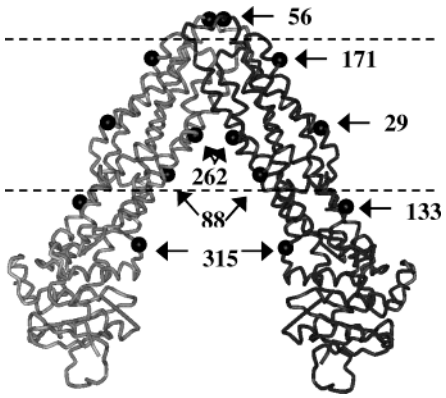

FIGURE 1: Crystal structure (4.5 Å resolution) of the *E. coli* MsbA homodimer (*11*) is shown with the introduced cysteine mutation sites indicated. MsbA is highly α-helical and consists mainly of a membrane spanning domain (top) and a nucleotide binding domain (bottom bundle). The predicted location of the membrane interface based on data presented here is also indicated (dashed lines).

RESULTS

The crystallographic structure of the MsbA homodimer is shown in Figure 1 along with the positions of the mutations studied here. Four sites along the putative dimer interface were chosen (F56C, A262C, C88, and C315) in order to confirm or refute the orientation found in the crystal structure, while three sites on the opposite faces of the transmembrane helices were selected (L171C, V29C, and E133C) in order to determine the positioning of the dimer within in the membrane bilayer.

EPR Spectra. The EPR spectra of the spin-labeled MsbA mutants reconstituted into inner membrane liposomes are shown in Figure 2. All of the spectra, with the exception of C315, show the presence of two distinct motional components, suggesting that the spin label side chains are able to adopt at least two different conformations relative to the protein or that there is a dynamic equilibrium between conformational states. All of the spectra except C315 exhibit at least some contribution from strongly immobilized spin label side chains, and this is particularly dominant in the F56, E133C, and L171C spectra. In addition, although most show a small population of a higher mobility component, the majority of spectra show at least some fairly strong immobilization of the spin label side chain. These results indicate that the spin label side chains on the chosen sites are not freely mobile but constrained by either neighboring side chains or tertiary contacts.

Accessibility Data. CW power saturation EPR spectroscopy has proven to be a convenient method for determining the local environment of introduced spin labels within a large protein structure. In addition, it is useful for integral membrane proteins, as depth of a given spin label side chain within a lipid bilayer can be determined using accessibility data to both oxygen and a water soluble paramagnetic broadening reagent such as NiEDDA and CROX. Oxygen and NiEDDA have inverse concentration gradients into the lipid bilayer, which enables the depth of the spin label from the phosphate groups of the lipids to be calibrated and measured. This allows the depth of a spin label attached to a transmembrane helix, for example, to be determined by measuring the accessibilities of the label to both oxygen and NiEDDA. This is an extremely useful technique for position-

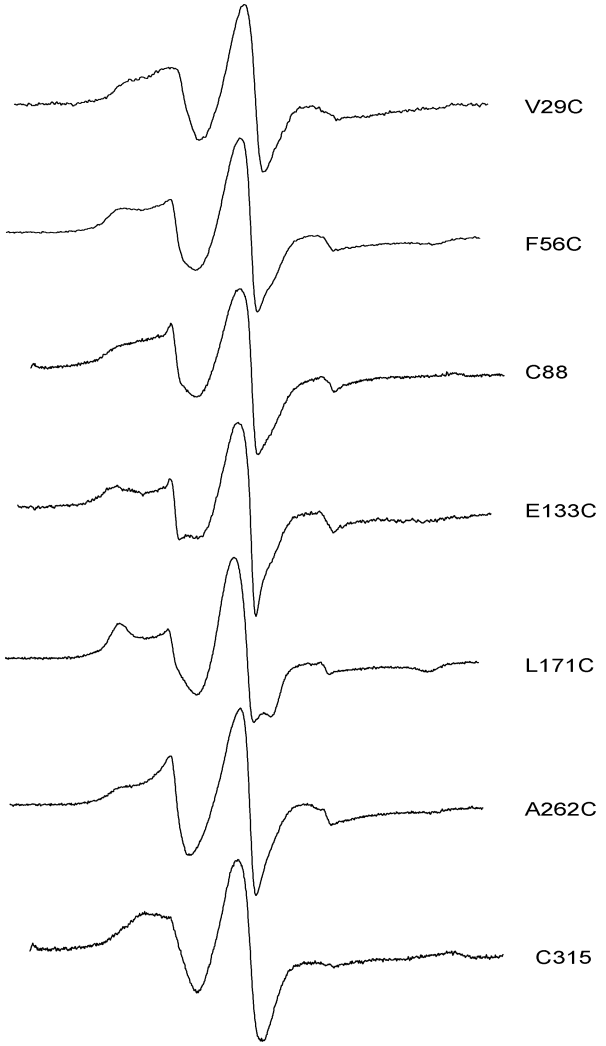

FIGURE 2: CW X-band EPR spectra of the MTSL-labeled MsbA mutants after reconstitution into inner membrane liposomes. All spectra were recorded at room temperature with a 100 G scan width, 10 mW microwave power, and a 50−100 μM protein concentration and are typically the average of 25−36 scans.

Table 1: Accessibility Parameters and Depth Calculations[a]

mutation	$\Delta P_{1/2}$ (O_2)[b]	$\Delta P_{1/2}$ (NiEDDA)	$\Delta P_{1/2}$ (CROX)	Φ	depth (Å)
V29C	8.66	3.10		1.03	8.9
F56C	7.38	9.01	10.77	−0.20	
C88	7.72	7.89	2.16	−0.02	3.9
E133C	6.96	11.78	6.48	−0.53	
L171C	5.31	5.10		0.04	4.2
A262C	10.85	2.94	2.13	1.31	10.2
C315	11.63	3.30		1.26	

[a] Power saturation parameters reflect accessibility and bilayer depth for spin-labeled MsbA cysteine mutants in liposomes. [b] $\Delta P_{1/2}$ parameters were obtained in the presence of air (20% oxygen), 200 mM NiEDDA, or 20 mM CROX, as described in the text. Φ values and subsequent depth measurements were calculated from eqs 1 and 2 (see text).

ing protein segments such as α-helices within the lipid bilayer (e.g., *28*, *29*, *35*) and is clearly applicable to the study of the recently crystallized MsbA.

The results obtained from the power saturation measurements are summarized in Table 1. The predicted membrane-exposed residues V29C, C88, L171C, and A262C were analyzed first. On the basis of the Φ values measured by

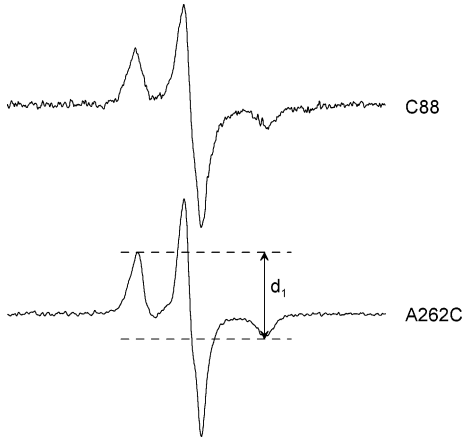

FIGURE 3: CW X-band spectra of 100 μM MsbA taken at 167 K are shown. Spectra were recorded with a 200 G scan width and a 2 mW microwave power, and signals were averaged 25−36 times. The d_1/d lineheight values were obtained where d_1 is the total height of the outer lines (as indicated) and d is the height of the center line.

EPR, site 171 is 4.2 Å deep into the membrane, while V29C is 8.9 Å deep. Residues C88 and A262C are 3.9 and 10.2 Å deep, respectively. These values are consistent with the six helix bundles being transmembrane, as predicted from the crystal structure. These depths also allow positioning of MsbA as a whole within the membrane bilayer, which was not previously possible.

It was predicted that the short helical section of MsbA, which contains residue E133C, is not membrane-exposed and serves as a linker region to the soluble NBD (*11*). Our results show that site E133C is located at the membrane interface, with accessibilities indicative of a mainly aqueous-exposed site. On the opposite side of the membrane, site F56C shows high accessibility to both reagents, indicative of a surface-exposed site.

To further establish that residues F56C and E133C were not embedded in the membrane, accessibility of these sites to 20 mM CROX, a charged reagent only found in the aqueous phase, was determined. F56C gave a $\Delta P_{1/2}$ (CROX) of 10.8, and E133C gave a $\Delta P_{1/2}$ (CROX) of 6.5, clearly indicating that these sites are indeed in the aqueous phase and not inserted into the membrane. As a control, the accessibility to CROX of the 5-doxyl PC spin label, which is 8 Å into the bilayer, reported a $\Delta P_{1/2}$ (CROX) value of only 0.5. In addition, the $\Delta P_{1/2}$ (CROX) accessibility values of about 2.1 for sites C88 and A262C further confirm that these sites were indeed located within the membrane and not within a water-filled cavity. Last, C315 was chosen at a location between the linker helices and the top of the NBD. Power saturation results show a high accessibility to oxygen but a lower exposure to NiEDDA than expected for a surface-exposed site.

Frozen Spectra. To help verify or refute that the dimer orientation was as shown in the crystal structure, the frozen (160 K) spectra of residues C88 and A262C were recorded (Figure 3). The d_1/d lineheight ratio is a qualitative measure of the extent of dipolar broadening due to spin−spin interaction between two spin label side chains (*36*). Values below 0.35 indicate little or no interaction, while d_1/d values above 0.40 indicate intermediate to strong interaction. For residues C88 and A262C, the d_1/d values were determined

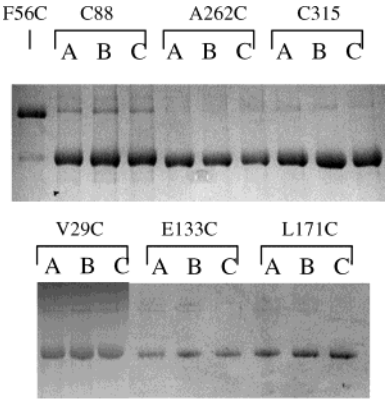

FIGURE 4: Five micrograms of each of the MsbA mutations shown were reacted with the following cross-linkers: (A) BMOE (8 Å spacer), (B) DTME (13 Å), and (C) DPDPB (20 Å) and analyzed by SDS−PAGE. Monomeric MsbA runs at approximately 65 kDa (lower bands), while cross-linked MsbA runs at about 130 kDa (upper bands).

to be 0.40 and 0.38, respectively, indicating weak dipolar interaction between these sites. Further evidence to suggest the spin labels indeed facing each other in the dimer structure is the fact that the d_1/d ratios decreased after the samples were solubilized in 2% SDS in order to break apart the dimers into monomers and eliminate the dipolar interactions between the labeled sites.

Cross-Linking Experiments. In addition to EPR distance measurements, chemical cross-linking was utilized as an additional approach for determining general distances between the monomers at each mutant location. The MsbA cysteine mutations were each reacted with three different chemical cross-linking reagents in order to estimate the distance between the monomers and their orientation with respect to each other. BMOE, DTME, and DPDPB each have spacers of 8, 13.26, and 19.9 Å, respectively. The results of the cross-linking of A262C, C88, and C315 are shown in Figure 4, where the covalently cross-linked monomers run as a dimer at ~130 kDa. F56C is not included in these studies since it is able to form spontaneous covalent dimers through disulfide bond formation and requires 500-fold excess β-mercaptoethanol and boiling to reduce the dimers to monomers. Therefore, Figure 4 shows only the spontaneous disulfide bonding results for F56C. As suggested by the crystal structure of MsbA (*11*) and its ability to spontaneously disulfide bond with itself, site F56C is in fact in very close contact in the resting state, while position C88 showed some ability to cross-link by all three linkers. Also, position C315 showed the ability to be cross-linked to a small extent, while A262C showed very little or no cross-linking. It was expected that the C_αs of A262C may be close enough for cross-linking to occur, especially with the 20 Å spacer. It may be that these side chains are in an unfavorable relative orientation with respect to each other and thus unavailable for cross-linking within the distance of the longest spacer arm used. That is, although the α-carbons themselves are close enough for cross-linking, the cysteine side chains may actually be pointing away from each other, adding to the distances between the sites, not shortening the distances. Without the aid of a more resolved crystal structure, the position of the side chains at this location is apparently not conducive to cross-linking.

In addition, the sites chosen on the outer face of the crystallographic dimer for depth measurements were also reacted with cross-linkers in order to exclude the possibility that the orientation observed in the crystal structure was inverted. The results of the cross-linking studies at L171C, V29C, and E133C are also shown in Figure 4. The small amount of cross-linking at site V29C is protein concentration-dependent, suggesting that this is a result of two dimers coming sufficiently close together to form a cross-link rather than a reorientation of the helical bundles. Consistent with the crystallographic arrangement of the resting state of the MsbA homodimer, none of the sites on the outer surface were able to be cross-linked to a great extent.

DISCUSSION

In this study, we have used SDSL EPR and chemical cross-linking methods to evaluate the resting conformation and membrane position of the *E. coli* MsbA homodimer. This is the first study to confirm the quaternary structural arrangement of the MsbA transmembrane helical bundles that was found in the crystal structure under more physiological conditions. The depth measurements from the SDSL experiments position the transmembrane domain of MsbA within the bilayer, leaving the tips of the helices exposed to the periplasm and the linker helices at the membrane interface. In addition, our results as shown here by chemical cross-linking and frozen state distance estimates by EPR are indeed consistent with the crystallographic homodimer conformation with residues A262C and C88 located on helices oriented toward each other, and the tips of the helical bundles (i.e., F56C) in close proximity.

Although all mutation sites were chosen on the outer surface of the protein, most of the spin-labeled spectra indicate that the spin label side chain attached to each site is fairly restricted in motion. This could be due to the fact that the low resolution of the crystal structure prohibited the selection of completely surface-exposed sites, or the packing of the amino acid side chains within the MsbA structure does not allow for unrestricted motion of the spin labels. Interactions with neighboring side chains may also explain the lowered accessibilities of the apparently surface-exposed C315 spin label.

Although depth measurements for F56C and E133C can be calculated using their Φ values, the CROX accessibilities rule out insertion into the bilayer. Because E133C is at the interface, it is possible, given the flexibility and length of the spin label side chain, that it may insert slightly into the phosphate headgroup region of the bilayer. The accessibility of F56C to CROX was high enough to rule out the possibility of any significant membrane insertion of the side chain, especially at the depth that would result from the reported $\Delta P_{1/2}$ values.

The question of whether the pocket created by the dimer interface was water-filled or membrane-exposed is now answered. Our power saturation depth measurements strongly indicate that the dimer interface residues A262C and C88 are exposed to the membrane, showing depths of 10 and 4 Å, respectively. These depth estimates are consistent with the conformation of the dimer shown in the crystal structure, and the low CROX accessibility of both of these sites further argues against a water-filled cavity. Having the entire

membrane spanning region accessible to the lipid bilayer is also consistent with the ability of MsbA to bind lipid A in the pocket of the homodimer prior to transport across the membrane.

Although only qualitative results concerning the proximity of the spin label pairs were obtained through frozen state EPR measurements, this was sufficient information to confirm the dimer orientation within the membrane. One thing to consider when analyzing dipolar interactions by frozen spectral samples is that if the protein is underlabeled, as in our case, it will significantly bias the spin−spin results toward weaker interactions, as not all spins are able to interact with another spin label. In addition, with the spin label arm length of approximately 6−7 Å and the α-carbons for the C88 and A262C pairs at 37 and 22 Å apart, respectively, in order for C88 and A262C side chains to show interaction, the spin label side chains must be oriented toward each other. However, because both of these sites are located on the outer surface of the protein and show a relatively mobile component in the spectra, it is likely that only a fraction of the label population is oriented toward its partner. With the crystal structure resolution of only 4.5 Å, the side chain orientations are not yet known for this protein, and it is possible that the side chains for C88 and A262C do not point toward each other in the dimer structure, resulting in weaker spin−spin interactions and little or no cross-linking. However, in the *V. cholera* MsbA structure (*12*), which is thought to be in the closed conformation, the side chains themselves at sites A262C and C315 are pointed directly toward each other. With attached spin labels, the distance between A262C and C315 in the closed structure would be approximately 5 and 2.5 Å apart, respectively, clearly suggesting that our lack of such significant interaction is consistent with MsbA being in the open conformation.

One drawback to cross-linking experiments is that they can covalently lock two cysteine sites together, even if they are only transiently close enough to be linked, biasing the results toward a conformation that only exists momentarily due to protein breathing or spontaneous formation of an excited state (without ligand) and may not reflect the actual resting state of the dimer. Conversely, information on possible excited state conformations may be gained with chemical cross-linking by locking those conformations that may only be transient and not otherwise observable. The small amount of cross-linking observed for C315 may be due to protein dynamics where the two monomers are caught in a transient state that brings the sites within close enough proximity for cross-linking to occur, trapping the intermediate state.

The recently solved MsbA crystal structures and the results of this study on *E. coli* MsbA in a lipid environment provide an excellent starting point for further structural dynamics analysis by SDSL on the mechanism of ligand binding and transport.

REFERENCES

1. Poole, K. (2003) Overcoming multidrug resistance in gram-negative bacteria. [Review]. *Curr. Opin. Invest. Drugs 4*, 128−139.
2. Leonessa, F., and Clarke, R. (2003) ATP binding cassette transporters and drug resistance in breast cancer. *Endocr.-Relat. Cancer 10*, 43−73.
3. Nachega, J. B., and Chaisson, R. E. (2003) Tuberculosis drug resistance: a global threat. *Clin. Infect. Dis. 36*, S24−S30.
4. Thomas, H., and Coley, H. M. (2003) Overcoming multidrug resistance in cancer: an update on the clinical strategy of inhibiting p-glycoprotein. *Cancer Control 10*, 159−165.
5. Tsuruo, T., Naito, M., Tomida, A., Fujita, N., Mashima, T., Sakamoto, H., and Haga, N. (2003) Molecular targeting therapy of cancer: drug resistance, apoptosis and survival signal. [Review]. *Cancer Sci. 94*, 15−21.
6. Kellen, J. A. (2003) The reversal of multidrug resistance: an update. *J. Exp. Ther. Oncol. 3*, 5−13.
7. Gottesman, M. M., and Ambudkar, S. V. (2001) Overview: ABC transporters and human disease. [Review]. *J. Bioenerg. Biomembr. 33*, 453−458.
8. Cotten, J. F., and Welsh, M. J. (1997) Covalent modification of the regulatory domain irreversibly stimulates cystic fibrosis transmembrane conductance regulator. *J. Biol. Chem. 272*, 25617−25622.
9. Chen, C. J., Clark, D., Ueda, K., Pastan, I., Gottesman, M. M., and Roninson, I. B. (1990) Genomic organization of the human multidrug resistance (MDR1) gene and origin of P-glycoproteins. *J. Biol. Chem. 265*, 506−514.
10. Dean, M., Hamon, Y., and Chimini, G. (2001) The human ATP-binding cassette (ABC) transporter superfamily. [Review]. *J. Lipid Res. 42*, 1007−1017.
11. Chang, G., and Roth, C. B. (2001) Structure of MsbA from *E. coli*: a homologue of the multidrug resistance ATP binding cassette (ABC) transporters. *Science 293*, 1793−1800.
12. Chang, G. (2003) Structure of MsbA from Vibrio cholera: a multidrug resistance ABC transporter homologue in a closed conformation. *J. Mol. Biol. 330*, 419−430.
13. Diederichs, K., Diez, J., Greller, G., Muller, C., Breed, J., Schnell, C., Vonrhein, C., Boos, W., and Welte, W. (2000) Crystal structure of MalK, the ATPase subunit of the trehalose/maltose ABC transporter of the archaeon *Thermococcus litoralis*. *EMBO J. 19*, 5951−5961.
14. Hung, L. W., Wang, I. X., Nikaido, K., Liu, P. Q., Ames, G. F., and Kim, S. H. (1998) Crystal structure of the ATP-binding subunit of an ABC transporter. *Nature 396*, 703−707.
15. Rosenberg, M. F., Kamis, A. B., Callaghan, R., Higgins, C. F., and Ford, R. C. (2003) Three-dimensional structures of the mammalian multidrug resistance P-glycoprotein demonstrate major conformational changes in the transmembrane domains upon nucleotide binding. *J. Biol. Chem. 278*, 8294−8299.
16. Hopfner, K. P., Karcher, A., Shin, D. S., Craig, L., Arthur, L. M., Carney, J. P., and Tainer, J. A. (2000) Structural biology of Rad50 ATPase: ATP-driven conformational control in DNA double-strand break repair and the ABC-ATPase superfamily. *Cell 101*, 789−800.
17. Fetsch, E. E., and Davidson, A. L. (2003) Maltose transport through the inner membrane of *E. coli*. *Front. Biosci. 8*, D652−D660.
18. Ames, G. F., Nikaido, K., Wang, I. X., Liu, P. Q., Liu, C. E., and Hu, C. (2001) Purification and characterization of the membrane-bound complex of an ABC transporter, the histidine permease. *J. Bioenerg. Biomembr. 33*, 79−92.
19. Karow, M., and Georgopoulos, C. (1993) The essential *Escherichia coli* msbA gene, a multicopy suppressor of null mutations in the htrB gene, is related to the universally conserved family of ATP-dependent translocators. *Mol. Microbiol. 7*, 69−79.
20. Zhou, Z., White, K. A., Polissi, A., Georgopoulos, C., and Raetz, C. R. (1998) Function of *Escherichia coli* MsbA, an essential ABC family transporter, in lipid A and phospholipid biosynthesis. *J. Biol. Chem. 273*, 12466−12475.
21. Karow, M., and Georgopoulos, C. (1993) The essential *Escherichia coli* msbA gene, a multicopy suppressor of null mutations in the htrB gene, is related to the universally conserved family of ATP-dependent translocators. *Mol. Microbiol. 7*, 69−79.
22. Campbell, J. D., Biggin, P. C., Baaden, M., and Sansom, M. S. P. (2003) Extending the structure of an ABC transporter to atomic resolution: Modeling and simulation studies of MsbA. *Biochemistry 42*, 3666−3673.
23. Thomas, P. J., and Hunt, J. F. (2001) A snapshot of Nature's favorite pump. *Nat. Struct. Biol. 8*, 920−923.
24. Higgins, C. F., and Linton, K. J. (2001) Structural biology. The xyz of ABC transporters. *Science 293*, 1782−1784.

25. Klug, C. S., and Feix, J. B. (2004) SDSL: A survey of biological applications, in *Biological Magnetic Resonance Volume 24* (Berliner, L. J., Eaton, S. S., and Eaton, G. R., Eds.) pp 269−308, Kluwer Academic/Plenum Publishers, Hingham, MA.
26. Klug, C. S., Su, W., and Feix, J. B. (1997) Mapping of the residues involved in a proposed beta-strand located in the ferric enterobactin receptor FepA using site-directed spin-labeling. *Biochemistry 36*, 13027−13033.
27. Hubbell, W. L., Cafiso, D. S., and Altenbach, C. (2000) Identifying conformational changes with site-directed spin labeling. [Review]. *Nat. Struct. Biol. 7*, 735−739.
28. Hubbell, W. L., Gross, A., Langen, R., and Lietzow, M. A. (1998) Recent advances in site-directed spin labeling of proteins. [Review]. *Curr. Opin. Struct. Biol. 8*, 649−656.
29. Isas, J. M., Langen, R., Haigler, H. T., and Hubbell, W. L. (2002) Structure and dynamics of a helical hairpin and loop region in annexin 12: a site-directed spin labeling study. *Biochemistry 41*, 1464−1473.
30. Doerrler, W. T., and Raetz, C. R. (2002) ATPase activity of the MsbA lipid flippase of *Escherichia coli*. *J. Biol. Chem. 277*, 36697−36705.
31. Gonzalez-Romo, P., Sanchez-Nieto, S., and Gavilanes-Ruiz, M. (1992) A modified colorimetric method for the determination of orthophosphate in the presence of high ATP concentrations. *Anal. Biochem. 200*, 235−238.
32. Altenbach, C., Flitsch, S. L., Khorana, H. G., and Hubbell, W. L. (1989) Structural studies on transmembrane proteins. 2. Spin labeling of bacteriorhodopsin mutants at unique cysteines. *Biochemistry 28*, 7806−7812.
33. Altenbach, C., Greenhalgh, D. A., Khorana, H. G., and Hubbell, W. L. (1994) A collision gradient method to determine the immersion depth of nitroxides in lipid bilayers: application to spin-labeled mutants of bacteriorhodopsin. *Proc. Natl. Acad. Sci. U.S.A. 91*, 1667−1671.
34. Dalton, L. A., McIntyre, J. O., and Flewelling, R. F. (1987) Distance estimate of the active center of d-b-hydroxybutyrate dehydrogenase from the membrane surface. *Biochemistry 26*, 2117−2130.
35. Zhao, M., Zen, K. C., Hernandez-Borrell, J., Altenbach, C., Hubbell, W. L., and Kaback, H. R. (1999) Nitroxide scanning electron paramagnetic resonance of helices IV and V and the intervening loop in the lactose permease of *Escherichia coli*. *Biochemistry 38*, 15970−15977.
36. Sun, J., Voss, J., Hubbell, W. L., and Kaback, H. R. (1999) Proximity between periplasmic loops in the lactose permease of *Escherichia coli* as determined by site-directed spin labeling. *Biochemistry 38*, 3100−3105.

BI0497751